Atmospheric Environment 44 (2010) 131–140

Contents lists available at ScienceDirect

Atmospheric Environment

journal homepage: www.elsevier.com/locate/atmosenv

Highly time- and size-resolved characterization of submicron aerosol particles in Beijing using an Aerodyne Aerosol Mass Spectrometer

Junying Sun [a,*,1], Qi Zhang [b], Manjula R. Canagaratna [c], Yangmei Zhang [a], Nga L. Ng [c], Yele Sun [b], John T. Jayne [c], Xiaochun Zhang [a], Xiaoye Zhang [a], Douglas R. Worsnop [c]

[a] Key Laboratory for Atmospheric Chemistry, Center for Atmosphere Watch and Services, Chinese Academy of Meteorological Sciences, China Meteorological Administration, Beijing 100081, China
[b] Atmospheric Sciences Research Center (ASRC), State University of New York, 251 Fuller Road, University at Albany, State University of New York, Albany, NY 12203, USA
[c] Center for Aerosol and Cloud Chemistry, Aerodyne Research Inc., 45 Manning Road, Billerica, MA 01821, USA

ARTICLE INFO

Article history:
Received 16 December 2008
Received in revised form
12 March 2009
Accepted 12 March 2009

Keywords:
Fine particles
Primary Organic Aerosol (POA)
Secondary Organic Aerosol (SOA)
Megacity
Air pollution
Size distribution
Aerosol sources and processes

ABSTRACT

Atmospheric aerosols are a major pollutant in Beijing—a megacity in China. To achieve a better understanding of the characteristics, sources and processes of aerosols in Beijing, an Aerodyne Aerosol Mass Spectrometer (AMS) was deployed at an urban site in July 2006 to obtain size-resolved chemical composition of non-refractory submicron particles (NR-PM_1) at 5 min resolution. During this study, NR-PM_1 was on average composed of 25% sulfate, 22% nitrate, 16% ammonium, 1.4% chloride and 35% of organic aerosol (OA) species. The average size distributions of sulfate, nitrate and ammonium were very similar and characterized by a prominent accumulation mode peaking at $D_{va} \approx 600$ nm. The average size distribution of OA was significantly broader due to the presence of an ultrafine mode. Multivariate analysis of the AMS organic spectra with Positive Matrix Factorization (PMF) identified a hydrocarbon-like OA (HOA) and two oxygenated OA (OOA) components. The HOA component likely corresponded to primary OA material associated with combustion-related emissions. The two OOA components, which likely corresponded to more oxidized (OOA I) and less oxidized (OOA II) secondary OA materials, accounted for 45 ± 16% and 16 ± 7.2%, respectively, of the observed OA mass. OOA I correlated well with sulfate while OOA II correlated well with nitrate. The particle loading, composition and size distributions observed during this campaign were highly variable. Backtrajectory analysis indicates that this variability correlated with the varying impacts of regional and local sources and processes.

1. Introduction

As the political and cultural center of China, Beijing has experienced unprecedented changes in the past two decades. Along with fast economical growth, air quality in Beijing has suffered severe deterioration, with particulate matter (PM) being one of the top pollutants (e.g., Chan and Yao, 2008; Duan et al., 2004; He et al., 2002, 2001). Recent studies indicate that a large mass fraction of ambient PM in Beijing is fine particles ($PM_{2.5}$), of which organics, sulfate, nitrate and ammonium are the major components. The major sources of $PM_{2.5}$ were identified to include coal burning, traffic exhausts, factory emissions, and biomass burning (Duan et al., 2004; Guinot et al., 2007; He et al., 2001; Zheng et al., 2005). Previous studies also reported dust particles as an important component of both $PM_{2.5}$ and PM_{10} in Beijing, especially in spring time due to the influences of dust storm events (e.g., Dillner et al., 2006; Sun et al., 2004).

Most aerosol chemistry studies in Beijing so far have been based on filter sampling that offers information at coarse time resolution and limited size separation. Online measurements are needed to capture fast variations in aerosol properties and to exploit correlations with high-time-resolution measurements and meteorological information to gain insights into aerosol sources and processes. In this study, an Aerodyne aerosol mass spectrometer (AMS) was deployed in Beijing in July 2006 to characterize the size-resolved composition of submicron particles (PM_1) every 5 min, aiming at understanding the physical and chemical processes leading to air pollution in Beijing.

In this paper, we discuss the concentrations, temporal variations, and size distributions of organics, sulfate, nitrate, ammonium, and chloride. The results of three organic aerosol (OA) components

* Corresponding author. Tel.: +86 10 68407943; fax: +86 10 62176414.
E-mail address: jysun@cams.cma.gov.cn (J. Sun).
[1] Also at State Key Laboratory of Cryosphere Sciences, Cold and Arid Regions Environmental and Engineering Research Institute, Chinese Academy of Sciences, Lanzhou 730000, China.

1352-2310/$ – see front matter © 2009 Elsevier Ltd. All rights reserved.
doi:10.1016/j.atmosenv.2009.03.020

determined via Positive Matrix Factorization (Paatero and Tapper, 1994) are presented. Finally the AMS results are correlated with air mass backtrajectories to examine the correlation between the observed variations in aerosol composition (and loading) and different source regions.

2. Experimental methods

2.1. Sampling site, meteorology, and instrumentation

This study was conducted on the campus of the Chinese Academy of Meteorological Sciences (CAMS) located in the northwest of Beijing between the 2nd and the 3rd ring roads (Fig. 1). Beijing is characterized as a semi-basin region with terrain decreasing gradually from northwest to southeast. The wind direction in Beijing is typically southern or southeastern in summer season, although weather conditions may change abruptly in association with passage of cold fronts. The average annual precipitation in Beijing is around 640 mm, of which most of the precipitation (70%) occurs in the summer.

Measurements of aerosol particles lasted continuously from 9 to 21 July 2006, except for occasional maintenance and calibration. Ambient air was sampled out of a window on the second floor (~5 m above ground level) of the CAMS building through a 3/8-inch copper tube (~4 m long). Coarse particles were removed using a cyclone with a 2.5 μm cutoff (model URG-2000-30EN, URG). A Quadrupole AMS (Aerodyne Research Inc.) was used to quantify size-resolved composition of PM_1 every 5 min. The number distributions of particles in $D_m = 10$–550 nm were measured every 5 min using a Scanning Mobility Particle Sizer (SMPS) system, which consists of an Electrostatic Classifier (TSI Model 3080), a bipolar ^{85}Kr aerosol neutralizer (TSI model 3077), a Long Differential Mobility Analyzer (TSI Model 3081), and a Condensation Particle Counter (TSI 3010). In addition, black carbon (BC) was measured every 1 min at the beginning of the study by a Multi Angle Absorption Photometer (MAAP; Thermo Model 5012).

2.2. AMS measurements and data analysis

Details of the AMS are presented in previous publications (e.g., Canagaratna et al., 2007). Only a brief description of the instrument and its operation is given here. In the AMS an aerodynamic lens is used to sample and focus ambient particles into a narrow beam that is transmitted to a heated surface (~600 °C) where particles are flash vaporized upon impact. The resulting vapor molecules are ionized by 70 eV electron impaction (EI), then, the positive ions are analyzed by a quadrupole mass spectrometer. Since the aerodynamic lens has reduced transmission efficiencies for particles at size of ~1 μm and since only non-refractory species (i.e., ammonium sulfate, nitrate, chloride and organics) evaporate at the vaporizer temperature (~600 °C), the AMS measurements represent non-refractory PM_1 (NR-PM_1) (Canagaratna et al., 2007).

During this study, the AMS alternated between the particle time-of-flight (pToF) mode and the mass spectra (MS) mode every 15 s. Under the pTOF mode operation, signals of eleven m/z's representative of NO_3^- (m/z 30 and 46), SO_4^{2-} (m/z 64 and 81), organics (m/z 43, 44, 55, and 57), NH_4^+ (m/z 16), H_2O (m/z 18), and N_2 (m/z 28) were recorded as a function of particle size. Reported mass concentrations and size distributions are the averages over periods of 5 min. The AMS was calibrated regularly for electron multiplier (EM) gain, ionization and ion transmission and detection efficiency (IE), and particle sizing following the standard protocols.

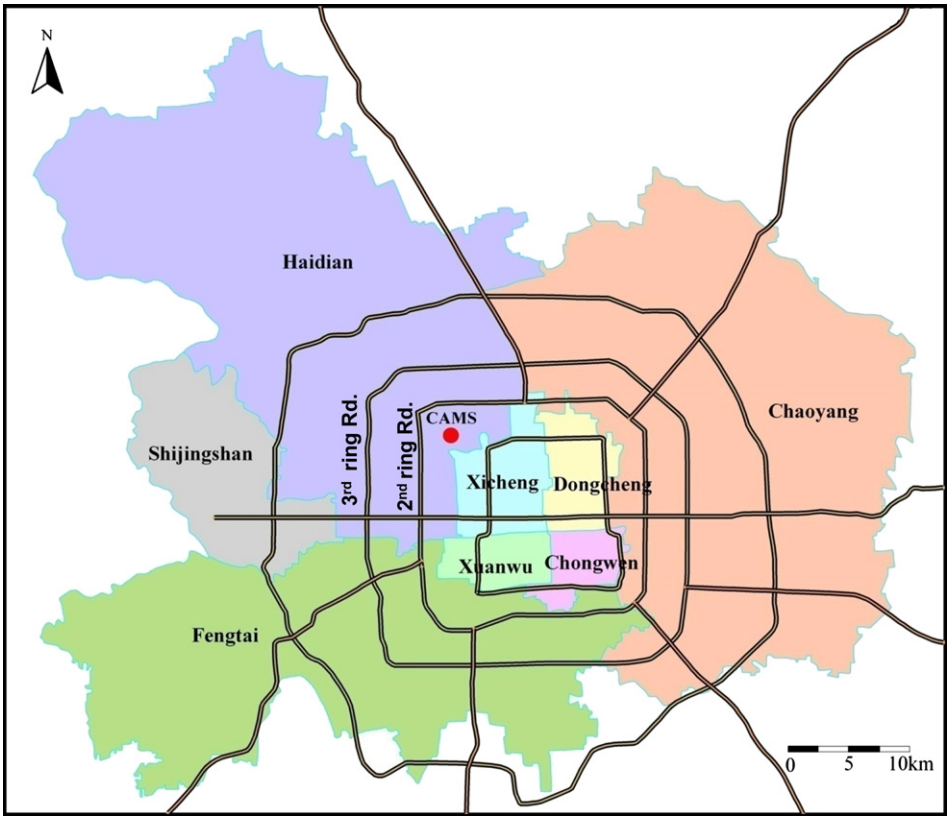

Fig. 1. Map showing Beijing city and the sampling site—CAMS (red solid circle). The city center is located in the center ring. (For interpretation of the references to color in this figure legend, the reader is referred to the web version of this article.)

Mass concentrations of each species were determined by summing up ion signals in the corresponding partial spectra using the fragmentation table approach described in Allan et al. (2004b). The measured AMS ion intensities are converted to mass concentrations using the average IE value (=1.91e−6) determined during this study and the default relative ionization efficiency (RIE) values (i.e., 1.2, 1.1, 1.3, and 1.4 for sulfate, nitrate, chloride, and organics, respectively). The RIE for ammonium (=4.6) was determined based on the analysis of pure ammonium nitrate particles.

The calculation of mass concentrations from AMS mass spectra also requires the use of a collection efficiency (CE) factor. Most field studies use a constant CE value (e.g., CE = 0.5) for ambient aerosol quantification and reported good agreements of measurements between AMS and collocated instruments (Drewnick et al., 2004; Salcedo et al., 2006; Takegawa et al., 2005; Zhang et al., 2005b). Recent studies have shown that CE values may be influenced by factors such as particle phase, composition, and water content (Allan et al., 2004a; Matthew et al., 2008). The water content of the sampled particles likely had the largest effect on the AMS CE during this campaign because the air conditioning inside the trailer caused condensation of liquid water in the inlet lines. The ratio between the AMS particulate H_2O signal and AMS total dry mass ($=SO_4^{2-} + NO_3^- + NH_4^+ + Cl^- +$ organics) was found to correlate with inlet RH when the ratio between the AMS-PM-H_2O and the AMS total dry mass increased beyond 0.4. Allan et al. (2004a) reported that the AMS CE for SO_4^{2-} containing particles approached 1 when RH in the sampling line was high and particles were likely in liquid form. Thus, the mass concentrations for this campaign were calculated with a CE = 0.5 except for time periods when AMS-PM-H_2O/AMS total dry mass > 0.4, then a CE = 1, consistent with Allan et al. (2004a), was used.

Fig. 2 shows a comparison between the AMS total dry mass calculated with the above CE values and the SMPS dry mass concentrations. The SMPS dry mass concentrations were obtained by converting the measured SMPS number distributions to volume distributions which were then integrated and corrected for estimated PM-H_2O content. The PM-H_2O measured by the SMPS was estimated to be a factor of 2.5 greater than the AMS-PM-H_2O mass. This factor accounts for the fact that approximately 60% of the original PM-H_2O content is lost due to evaporation in the aerodynamic lens inlet of the AMS (private communication with Slowik et al.; see also, Zelenyuk et al., 2006). SMPS volume was then converted to dry mass concentrations by applying dry particle densities estimated from the densities of $(NH_4)_2SO_4$, NH_4NO_3, and bulk organics (i.e., 1.8, 1.7 and 1.3 g cm^{-3}, respectively) weighed by their relative concentrations based on the AMS data (Varutbangkul et al., 2006; Zhang et al., 2005b). The calculated dry density varied from 1.33 to 1.70 g cm^{-3} with a mean value of 1.59 g cm^{-3} during this study. Note that since refractory species such as BC, metals and crustal components, are not considered in this calculation, the estimated dry density may contain systematic errors. While systematic errors between the AMS and SMPS mass concentrations may exist, the consistent correlation and reduction of outliers in Fig. 2 when compared with Fig. S1 in the supporting information, indicates that most of the variations in AMS CE have been taken into account by using the water content dependent variable CE.

The detection limits of the AMS measurements of mass concentration are evaluated on the basis of the mass spectra of particle-free ambient air. They are defined as 3 times the standard deviation of the corresponding species signals in the filtered air (Zhang et al., 2005b). The detection limits of sulfate, nitrate, ammonium, chloride, and organic during this study are estimated at 0.015, 0.01, 0.06, 0.03, and 0.06 μg m^{-3}, respectively, for a 5 min averaging time.

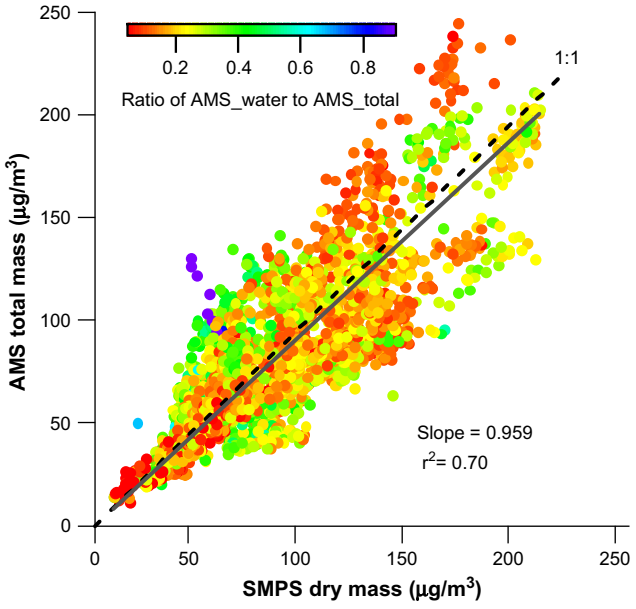

Fig. 2. Scatter plot of the AMS total NR-PM_1 mass vs. the SMPS dry mass.

2.3. Back trajectory analysis and air mass classification

In an effort to classify in general terms the source regions affecting the sampled aerosol particles, 48-h backtrajectories at 500 m arrival height above ground level were computed every 2 h starting at midnight Beijing time using the HYbrid Single Particle Lagrangian Integrated Trajectory (HYSPLIT-4) model developed by NOAA/ARL (Draxler and Rolph, 2003). The 2-day air mass histories of specific aerosol events observed with the AMS were examined by selecting backtrajectories for the time that most closely corresponded to the mean time of each aerosol event.

3. Results and discussion

3.1. Submicron aerosol characteristics

3.1.1. Mass concentrations and temporal variations of NR-PM_1 species

Fig. 3 shows the time series of the mass concentrations of SO_4^{2-}, NO_3^-, NH_4^+, organics, and Cl^- along with meteorological parameters (e.g., temperature, RH, wind speed and direction and precipitation). The weather conditions during this study were characterized with high temperature (hourly average 24.0–35.8 °C), high humidity (hourly average 26%–96%), and predominantly southern, southeastern wind at low speed (hourly average 0.03–4.2 m s^{-1}). These conditions were considered typical for Beijing in July (Zhuang et al., 1999).

The statistics of the mass concentrations of each species are shown in Table 1. Organics, sulfate, and nitrate were the major aerosol components. The average ($\pm 1\sigma$) composition of NR-PM_1 during this study was 35% (±18%) organics, 25% (±14%) sulfate, 22% (±16%) nitrate, 16% (±9%) ammonium, and 1.4% (±1.4%) chloride. The presence of substantial amounts of particulate nitrate in summer is interesting since NH_4NO_3 is relatively volatile and tends to dissociate and remain in the gas phase under high temperature. The average fraction of NO_3^- in NR-PM_1 in Beijing is approximately 2 times higher than the average value (~10%) observed in a number of urban locations during summer (Zhang et al., 2007a). A possible reason for the detection of large quantities of particulate nitrate in July is that there was plenty of NH_3 gas in the air to neutralize

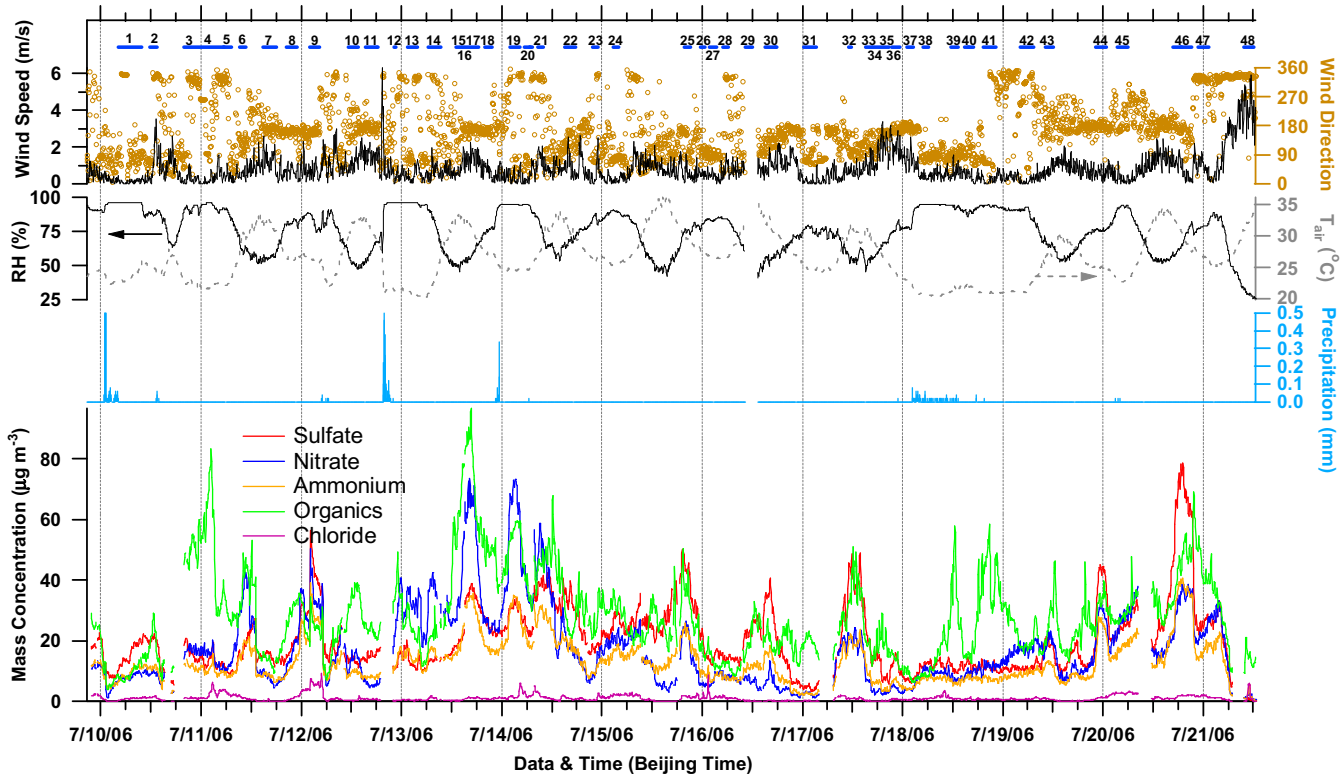

Fig. 3. Time series of the mass concentrations of sulfate, nitrate, ammonium, organics and chloride measured by the AMS and the meteorological parameters during 9–21 July, 2006 in Beijing. 48 events are marked as references for Figs. 10 and S3 & S4 in the supporting information.

H_2SO_4 and HNO_3, which is consistent with the observation that the measured particles appear to be bulk neutralized (see Section 3.1.2). In addition particles in Beijing were likely to be hydrated due to high RH, which may facilitate the absorbance of HNO_3 and NH_3 (Guinot et al., 2007; Sciare et al., 2007).

The total mass concentrations of NR-PM_1 ($=SO_4^{2-} + NO_3^- + NH_4^+ + Cl^- +$ organics) varied by a factor of ~22, from a minimum of 11.2 μg m^{-3} to a maximum of 245 μg m^{-3} (Table 1). The chemical composition of NR-PM_1 also varied substantially and dynamically (Fig. 3). The most abundant NR-PM_1 species was sometimes NO_3^- (e.g., July 14, 2:00–9:00), sometimes SO_4^{2-} (e.g., July 20 16:00–21:00), and more often organics (e.g., July 19). In addition, similar to observations by Streets et al. (2007), particles during this study usually built up under stagnant meteorological conditions over the course of several days followed by quick removal associated with heavy rain falls and/or the arrival of cleaner air from north (Fig. 3).

The NR-PM_1 chemical species show significantly different diurnal patterns with respect to each other during this study (Fig. 4). SO_4^{2-} had a pronounced diurnal profile that peaks in the late afternoon, which could be driven by enhanced photochemical production and condensation of gaseous H_2SO_4. Other factors, such as prevailing south winds and elevated temperature and RH during daytime, could have played a role as well since most of the emission sources of SO_2 and other air pollutants are located to the south of Beijing while regions to the north of Beijing have relatively fewer sources (Ohara et al., 2007). The wind patterns in Beijing in summer typically switch from southerly wind from noon to midnight to northerly wind from midnight to the next day's noon (Hu et al., 2005).

The diurnal curve of nitrate was relatively flat, which could be the outcome of two competing factors—enhanced volatilization of particulate ammonium nitrate and enhanced photochemical production of nitrate in the afternoon. The observed diurnal profile of chloride that peaks in the early morning, drops after 9 am, and stays at low levels between 12:00and 18:00 was likely partially driven by the gas–particle partitioning of ammonium chloride precursors (i.e., gaseous HCl and NH_3), which is favored by the lower temperature and higher RH during night and in early morning.

It is interesting to note that the average mass concentrations of organics shows two peaks, one in the early afternoon (12:00–13:00) and one in the evening (19:00–20:00). This is unlike the situations often seen in other urban locations, e.g., Pittsburgh (Zhang et al., 2005b), New York City (Drewnick et al., 2004) and Mexico City (Salcedo et al., 2006), where a morning peak of OA that correlates with morning traffic was typically observed. This unique variation was likely related to combined influence from local emissions, secondary production, transport and the evolution of boundary layer height (BLH).

Table 1
Summary of mass concentrations (μg m^{-3}) of NR-PM_1 species in Beijing, July 2006.

	Total	Sulfate	Ammonium	Nitrate	Chloride	Organics
Mean	80.0	20.3	13.1	17.3	1.1	28.1
1σ	40.6	11.6	7.4	13.2	1.1	14.8
Median	76.6	18.6	12.1	15.4	0.97	26.8
Minimum	11.2	0.23	0.27	0.5	< D.L.	1.2
Maximum	245	82.3	42.7	79.2	11.9	99.9

3.1.2. *Acidity of submicron particles*

Understanding acidity in atmospheric particles is important since it is a key parameter affecting aerosol hygroscopic growth, toxicity, and heterogeneous reactions. The acidity in NR-PM_1 in this study was examined by comparing the NH_4^+ mass concentration measured by the AMS to the amount needed to fully neutralize the anions that were measured:

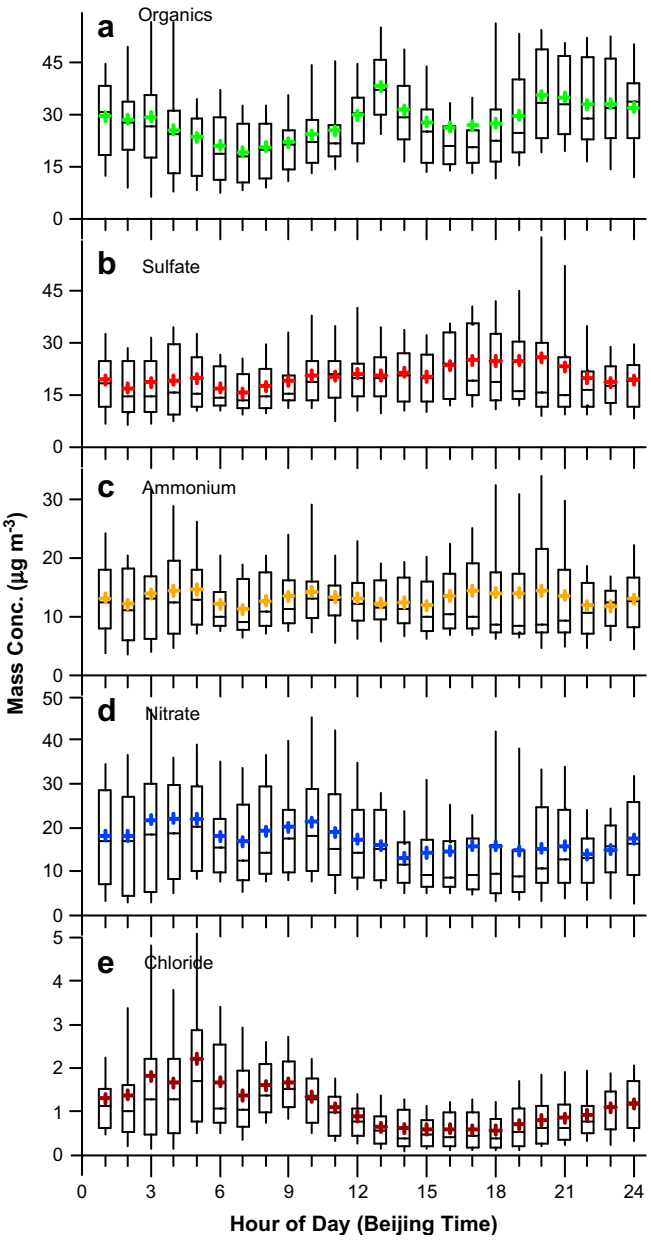

Fig. 4. Diurnal variation box plots of a) organics, b) sulfate, c) ammonium, d) nitrate and e) chloride. The box plots are read as follows: the upper and lower boundaries of the box indicate the 75th and the 25th percentiles, the line within the box marks the median, and the whiskers above and below the box indicate the 90th and 10th percentiles. Cross symbols represent the means. The *x*-axis labels of the diurnal plots correspond to the hour of the day, e.g., "1" means from 00:00 to 01:00 am.

$$NH_{4\,predict}^{+} = 18 \times \left(2 \times SO_4^{2-}/96 + NO_3^{-}/62 + Cl^{-}/35.5\right) \quad (1)$$

where SO_4^{2-}, NO_3^{-}, and Cl^{-} represent the mass concentrations (in μg m^{-3}) of the species; the denominators correspond to their molecular weights; and 18 is the molecular weight of NH_4^+. Particles are considered as "more acidic" if the measured NH_4^+ concentration is significantly lower than NH_4^+ predict and as "bulk neutralized" if the two values are similar. This approach is valid as long as the influence of metal ions and organic acids and bases on NH_4^+ predict is negligible (Zhang et al., 2007b). Note that dust and crustal materials only account for a small fraction (<10%) of the $PM_{2.5}$ mass in Beijing during summer months (e.g., He et al., 2001; Sun et al., 2004) although their concentrations could be much higher in spring (Dillner et al., 2006). Nevertheless, since the AMS does not detect materials nonvolatile at its higher temperature (~600 °C), the SO_4^{2-}, NO_3^{-}, and Cl^{-} concentrations measured by the AMS unlikely contain those bonded to metal cations (e.g., Na^+, Ca^{2+}, K^+, and Mg^{2+}) in dust, sea salt, and crustal materials. In addition, we estimated organic acid concentrations based on the AMS *m/z* 44 (CO_2^+) signal using an approach described in Zhang et al. (2007b). Organic acids were negligible compared to inorganic anions (~3% the molar equivalent concentrations of $SO_4^{2-} + NO_3^{-} + Cl^{-}$) during this study. We are therefore confident that our acidity estimation is applicable to Beijing.

The correlation between measured and predicted NH_4^+ was very tight ($r^2 = 0.98$) with a regression slope close to 1 (Fig. 5), indicating that PM_1 in Beijing was bulk neutralized for this measurement period. This conclusion is consistent with the observation of substantial amounts of particulate nitrate, which generally decreases with particle acidity and was found almost depleted in particles more acidic than ammonium bisulfate (Zhang et al., 2007b). Note that a study in 2001 reported that ammonium in particles of all sizes in Beijing was insufficient to neutralize measured nitrate and sulfate (Dillner et al., 2006). Our observation of particles being overall neutralized in 2006 could be due to the substantial reductions of SO_2 emissions in Beijing and adjacent cities in recent years, as part of the air pollution control measures initiated by the Chinese government (He et al., 2002, Beijing Environmental Statement 2003–2006, http://www.bjee.org.cn/news/index.php?ChannelID=138). Note that although increases in NH_3 emissions could also be a reason for more neutralized particles, we are unaware of published data supporting this possibility.

3.1.3. *Size distribution of NR-PM$_1$ species*

Fig. 6 shows the average size distributions of NR-PM_1 species and their percent contribution to the total mass over the entire campaign. Chloride was not included since neither of its major ion fragments was scanned for pToF during this study. However given

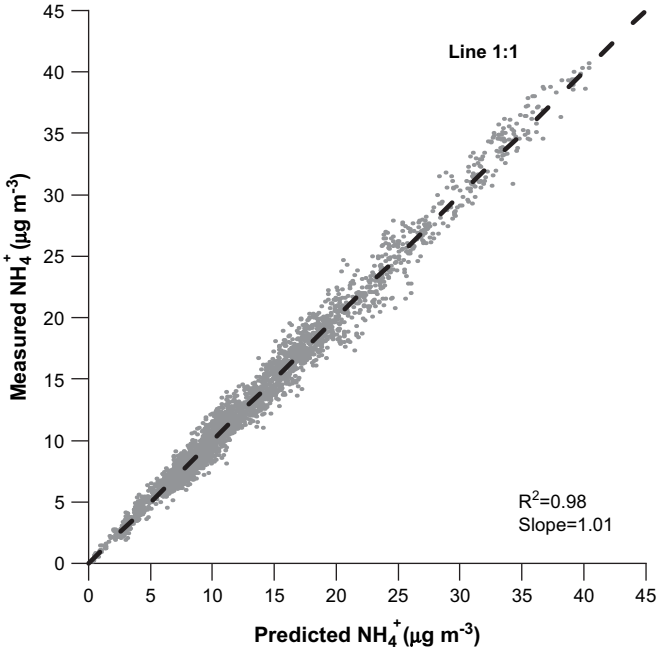

Fig. 5. Scatter plot that compares predicted NH_4^+ vs. measured NH_4^+. Predicted NH_4^+ was calculated based on the sulfate, nitrate, chloride concentrations measured by the AMS assuming they were fully neutralized by NH_4^+ (see Equation (1)).

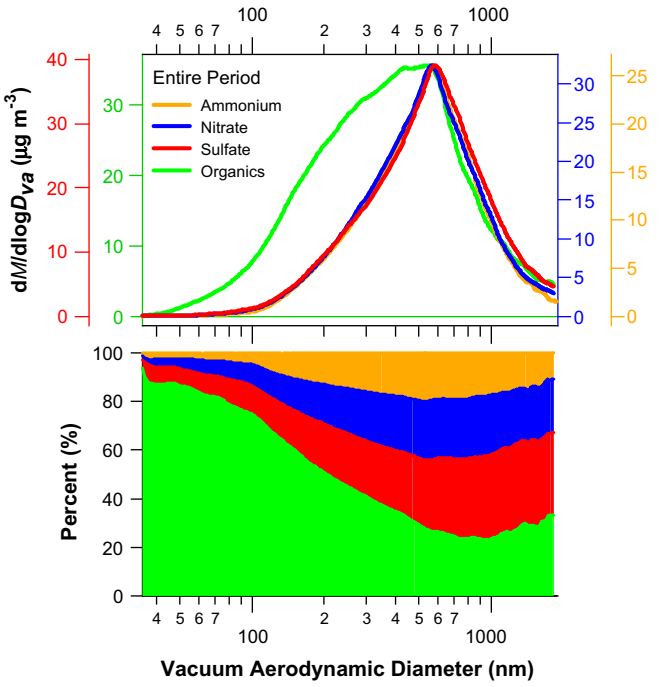

Fig. 6. Average chemically speciated size distributions and size-resolved percent fraction of chemical compositions of aerosols measured by the AMS.

its low concentrations (~1.4% of the NR-PM_1; Table 1), the influence of this species on the total size distribution should be negligible. The size distributions of inorganic species were very similar, showing a major accumulation mode peaking at a vacuum aerodynamic diameter (D_{va}; DeCarlo et al., 2004) at ~600 nm. This observation, together with the good correlations among species for their mass concentrations in the accumulation mode size range, implies that NH_4^+, SO_4^{2-}, and NO_3^- were likely internally mixed in the accumulation mode. Organic species showed a much broader size distribution and were increasingly more important in smaller particles. On average, 70%–90% of the ultrafine particle mass (D_{va} < 100 nm) was organic. In general, particles smaller than 200 nm were predominately organic, while the accumulation mode particles were dominated by sulfate and nitrate in Beijing. The enrichment of organics in smaller particles is frequently observed at urban locations (e.g., Allan et al., 2003; Alfarra et al., 2004; Zhang et al., 2005c). It is consistent with findings that the ultrafine particles in urban environments are primarily associated with local combustion emissions (Zhang et al., 2005c) while the larger mode is indicative of aged regional particulates containing mixed inorganic and organic species (e.g., Alfarra et al., 2004; Zhang et al., 2005c).

3.2. Organic aerosol components

Organic species were apparently an important aerosol component in Beijing, accounting for 16%–93% of the NR-PM_1 mass during this campaign. The average OA concentration in Beijing (28.1 μg m^{-3}; Table 1) was more than three times the value measured in a dozen of urban environments (Zhang et al., 2007a). In order to better understand the chemical composition and sources of OA in Beijing, we analyzed the AMS mass spectral matrix of OA with Positive Matrix Factorization (PMF, Paatero and Tapper, 1994) using the analysis and evaluation tool described by Ulbrich et al. (2009). The mass concentrations and mass spectra of three distinct components, including one hydrocarbon-like OA (HOA) and two oxygenated OA (OOA I and OOA II), were determined (Fig. 7). Taken together the three factors account for 98.4% of the measured organic mass. Increasing the number of factors appears to result in an apparent splitting of the HOA factor (Ulbrich et al., 2009) and does not improve the PMF fit significantly. The splitting of the HOA factor

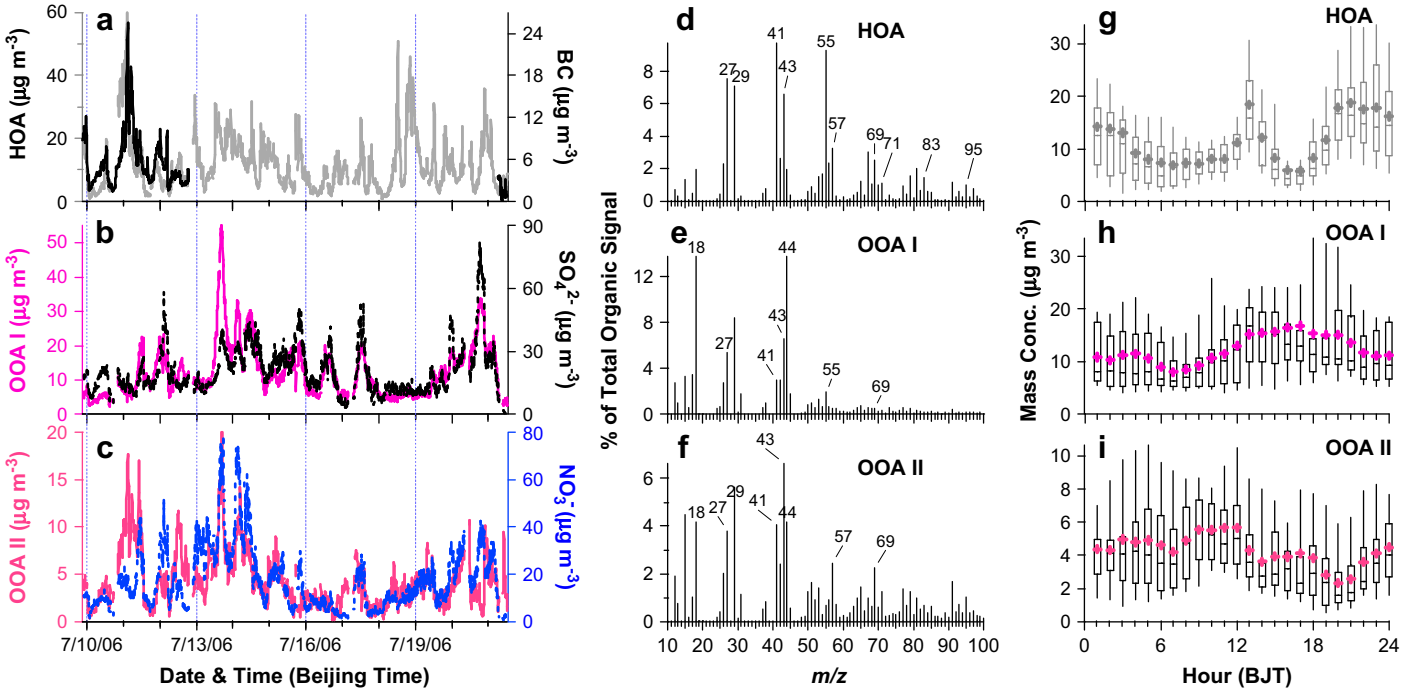

Fig. 7. Time series of the mass concentrations of a) HOA and BC, b) OOA I and sulfate, and c) OOA II and nitrate. Mass spectra of d) HOA, e) OOA I, and f) OOA II. Diurnal variation box plots of g) HOA, h) OOA I, and i) OOA II. The box plots are read as follows: the upper and lower boundaries of the box indicate the 75th and the 25th percentiles, the line within the box marks the median, and the whiskers above and below the box indicate the 90th and 10th percentiles. Cross symbols represent the means.

likely represents the variability in the POA sources that affect the observed aerosol. Due to the lack of co-located measurements, it was not possible to correlate the split HOA factors with possible POA sources. Thus, the three-factor solution was chosen for this analysis.

The HOA component correlated well with BC (Fig. 8a) and showed a mass spectrum dominated by peaks characteristic for hydrocarbons, such as $C_3H_5^+$ (*m/z* 41), $C_3H_7^+$ (*m/z* 43), $C_4H_7^+$ (*m/z* 55) and $C_4H_9^+$ (*m/z* 57) (Fig. 7d). Components classified as HOA were frequently observed in urban atmospheres (Zhang et al., 2005a,c, 2007a; Lanz et al., 2007; Ulbrich et al., 2009), most of which showed similar mass spectral pattern to those of diesel vehicle exhaust and lubricating oil aerosols (Canagaratna et al., 2004). While the HOA MS determined for this study was overall similar to the MS of diesel PM and HOA components for urban particles, it showed a somewhat higher ratio of $C_nH_{2n-1}^+$ (e.g., *m/z* 55) to $C_nH_{2n+1}^+$ (e.g., *m/z* 57; see Fig. S2 in the supporting information). In addition, the diurnal pattern of HOA contained a prominent peak between noon and 1 pm (Fig. 7g) which was rarely seen in other urban locations. Usually the diurnal curves of urban HOA show a peak in the morning around rush hours and a minimum during the daytime due to increase of BLH (Zhang et al., 2005c; Lanz et al., 2007; Ulbrich et al., 2009). Note that very similar diurnal pattern and MS of HOA were observed again in Beijing during summer 2008, suggesting that it is a typical phenomenon in Beijing during summertime and that other POA sources, such as cooking, in addition to traffic emissions might have contributed significantly to the observed HOA in Beijing.

The MS of both OOA components showed the characteristic features of oxidized organic material, e.g., a major peak at *m/z* 44 (CO_2^+, Alfarra et al., 2004; Zhang et al., 2005a). Differences in the intensity of *m/z* 44 fragment, however, reflect the different levels of oxidation in these two OOA components. To be consistent with previous studies (Lanz et al., 2007; Ulbrich et al., 2009), the more oxidized component was referred to as OOA I while the less oxidized component as OOA II. As shown in Fig. 8, the time series of total OOA (OOA I + OOA II) correlated well ($r^2 = 0.69$) with the sum of sulfate and nitrate—two well known secondary aerosol species, indicating that both OOA components were likely representative of SOA. For reference, HOA had almost no correlation with $SO_4^{2-} + NO_3^-$ ($r^2 = 0.033$), consistent with the assumption that HOA was likely a surrogate for combustion-related POA.

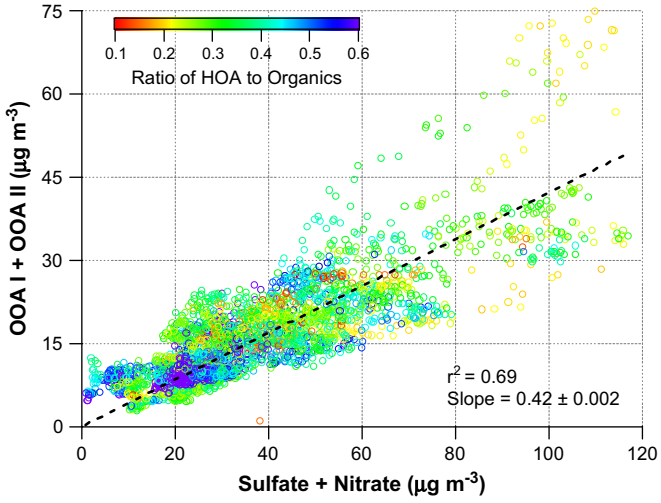

Fig. 8. Scatter plot of total OOA (=OOA I + OOA II) vs. total inorganic anions (=SO_4^{2-} + NO_3^-). The data points are colored by the ratio of HOA to total organics. (For interpretation of the references to color in this figure legend, the reader is referred to the web version of this article.)

The OOA I and OOA II components demonstrated good correlations with SO_4^{2-} and NO_3^-, respectively (Fig. 7b and c). The good correlation between OOA I and SO_4^{2-} was observed in various urban and rural/remote atmospheres, indicating the connection of OOA I to aged regional SOA (Zhang et al., 2005a,c, 2007a; Lanz et al., 2007; Ulbrich et al., 2009). On the other hand, previous studies in Pittsburgh (Ulbrich et al., 2009) and Switzerland (Lanz et al., 2007) have shown an OOA II component that correlated well with ammonium nitrate, suggesting that the OOA II observed in this campaign could correspond to semi-volatile SOA species.

3.3. Insights into submicron aerosols sources and processes in Beijing during summer

Dynamic variation in composition and size distribution is one of the key features of the ambient PM observed during this campaign. As shown in Fig. 3, substantial changes in aerosol loading and composition occurred on time scale of minutes to hours. Large spikes in OA loading occurred frequently while the increases of sulfate and nitrate appeared to be more gradual and usually lasted for a few days.

The observed temporal changes in aerosol loading and properties were the outcome of combined influences of various source emissions and atmospheric processes. Correlations between aerosol properties and meteorological variables may offer insights into potential sources and processes that may have affected the observed aerosol particles. In order to correlate aerosol properties to air mass source regions, we selected 48 events for periods when the chemical composition of NR-PM_1 was relatively constant and the meteorological conditions (e.g., wind direction) were stable (the events are marked on the top of Fig. 3). The average loading, composition and size distribution were determined for each event (see Figs. S3 and S4 in the supporting information) and their variations were correlated with air trajectories.

3.3.1. Case study of variability in aerosol size and composition

Fig. 9 provides an example of the type of variation observed on a typical day—July 11—during this campaign. On this day, the increases in HOA, OOA, sulfate and nitrate concentrations were largely independent of each other and reflected the changing effects of meteorology and processing on the ambient PM at the measurement site. Increases in HOA concentration were observed after midnight, between noon and 1 pm, and in late evening, together with enhancements of a small particle mode that is often a signature in AMS measurements of POA sources. The link between increasing HOA concentrations and the presence of an enhanced small particle mode was also observed during events 3, 31, 39, and 41 (Figs. S3 and S4).

The variability in NO_3^- concentrations and size distributions was consistent with the semi-volatile behavior expected for NH_4NO_3. In particular, NO_3^- concentration peaked in late morning with a broader size distribution, likely due to enhanced photochemical production of HNO_3 and elevated emission of primary aerosol that provided surfaces for gas-to-particle partitioning. In contrast, the lower NO_3^- concentrations observed during mid-day were likely the result of higher air temperature that favors evaporation of NH_4NO_3.

A change in wind direction from SW to S occurred around noon time on this day (Fig. 3), led to an abrupt decrease in all aerosol species (Fig. 9). The aerosol loading remained relatively stable during Event 7 and gradually increased again during Event 8. The size distributions of sulfate and OA during Events 7 and 8 were dominated by a mode centered at 500 nm, suggesting that much of the increase was due to transport of aged regional aerosol. The shapes of the size spectra of all species were very similar during Events 7 and 8, further suggesting that all aerosol species were

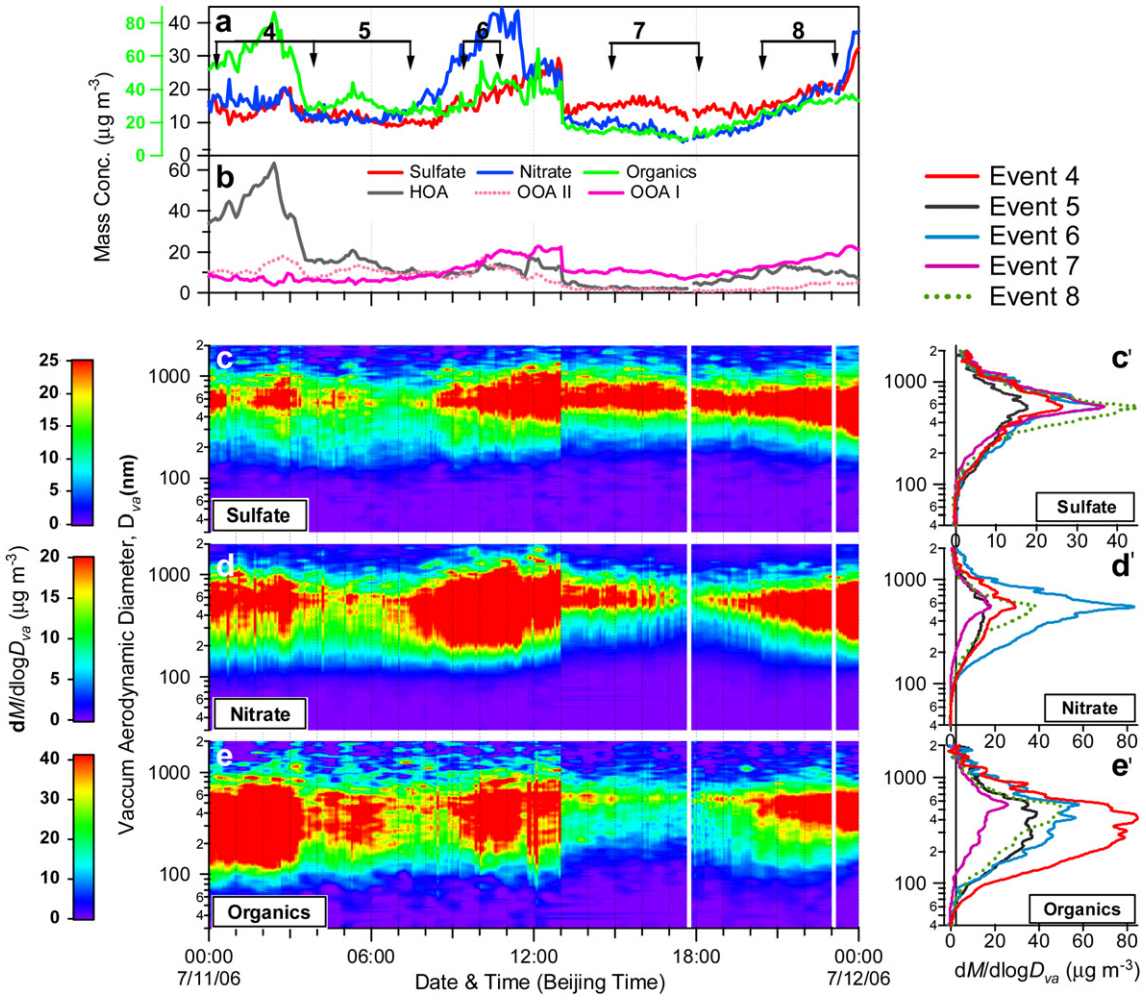

Fig. 9. Evolutions of a) organics, sulfate, and nitrate mass concentrations, b) HOA, OOA I, and OOA II concentrations, and c–e) the size distributions of sulfate, nitrate, and organics during July 11, 2006. To the right of the image plots are the average size distributions of corresponding species during events 4, 5, 6, 7, and 8 (for which the time periods are marked on a).

internally mixed in this regional aerosol mode. The dominance of an accumulation mode consisting of secondary organic and inorganic species was witnessed throughout this campaign and was particularly clear during Events 19, 21, and 46 (Figs. S3 and S4).

3.3.2. *Backtrajectory (BT) analysis*

Fig. 10 summarizes the correlations between NR-PM_1 characteristics and meteorological variables for the 48 distinct time periods identified for this study. The average compositions of NR-PM_1 during these periods and their speciated size distributions were highly variable as presented in Figs. S2 and S3. The corresponding BT can be broadly classified into 5 groups based on the directions: north (Group I), northwest (Group II), southwest (Group III), south (Group IV), and east (Group V). Only one BT was classified as Group I and two as Group II, due to the infrequency of northern flows in summer. Over 80% of the BT originated from S and SE, reflecting the typical summertime meteorology in Beijing. Specifically, since the topography of the Beijing urban area is generally flat with surrounding mountains on all sides except the south, the wind pattern over the Beijing area in summer is prevailing southern and southeastern, especially in daytime (Hu et al., 2005).

Although the statistical significance of our BT analysis may be limited due to relatively small number of the events, the correlations between aerosol properties and trajectories nevertheless signify the impacts of various source regions on aerosol pollution problems in Beijing. The highest aerosol loading and the largest fraction of secondary species (i.e., SO_4^{2-}, NO_3^-, NH_4^+, OOA I and OOA II) were observed in air masses arrived at the measurement site from the NW and S directions (Groups II and IV). The average size distributions among different aerosol species were also more similar for these two groups compared to the others (Figs. 10 and S3). These observations were likely indicative of the important contributions of pollutants emitted from densely populated, industrialized regions located to the S and the large point sources of emissions to the NW of Beijing (Ohara et al., 2007 and private communication with Dr. Cao Guoliang et al.).

Since the Groups III and IV trajectories were the shortest, aerosol observed during the corresponding periods likely had received the largest impacts from emissions in the city of Beijing and its immediate vicinity. The relatively larger fraction of nitrate suggested a significant impact of local NO_x emissions on aerosol pollution in Beijing. In addition, although the average aerosol compositions for Group V (E) and Group II (NW) were very similar, the average NR-PM_1 loading for Group II was approximately 2.5 times higher than that for Group V (145 μg m^{-3} vs. 60 μg m^{-3}; Fig. 10). Since the Group II aerosol contained the highest portion of sulfate observed during this study, it is likely that large point sources of SO_2, such as coal mining factories and coal-fired power

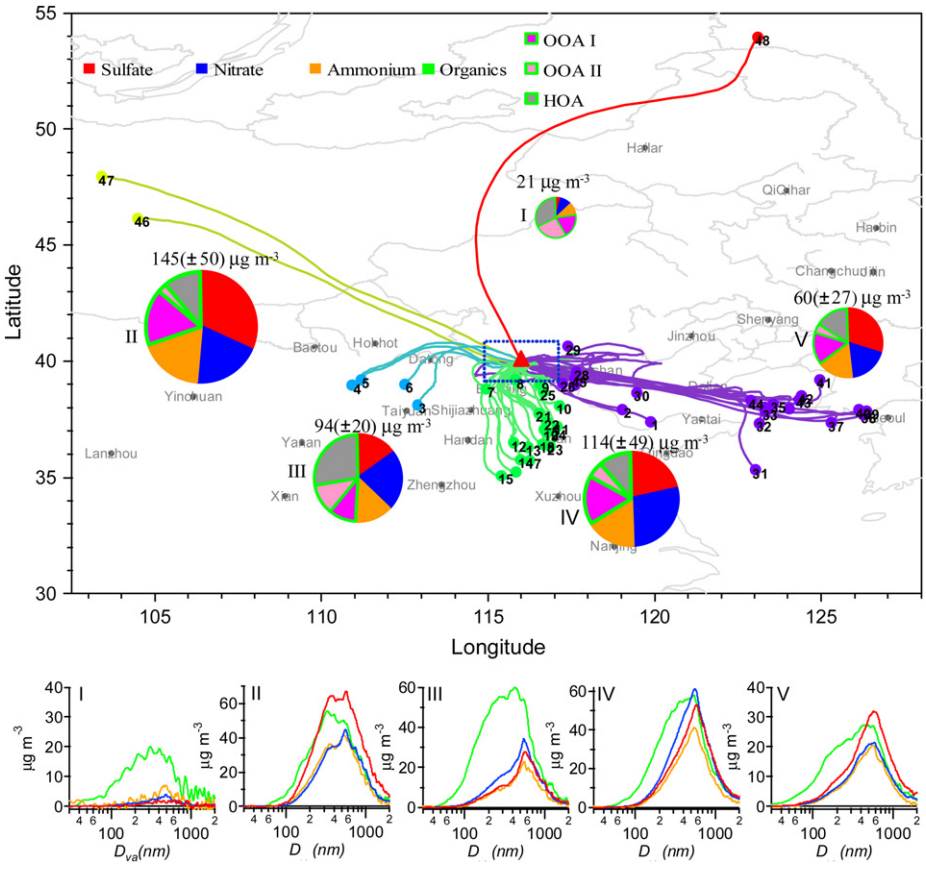

Fig. 10. The 48-h backtrajectories calculated using the NOAA HYSPLIT model for the 48 events selected for the study period (see Fig. 3 for the time periods of these events). The backtrajectories are classified into 5 clusters colored as such: I in red, II in olive, III in turquoise, IV in green, and V in purple. The average compositions of NR-PM_1 associated with each cluster are shown in the pie charts. Areas of the pie charts are scaled by the average NR-PM_1 concentrations marked on the top of the pies, the numbers in the parenthesis are 1σ of variation. The average size distributions of sulfate, nitrate, ammonium and organics for each cluster are shown at the bottom of the panel. The blue rectangle boarded around Beijing indicates the resolution of the HYSPLIT model (i.e., 191 km × 191 km). (For interpretation of the references to color in this figure legend, the reader is referred to the web version of this article.)

plants in the Shanxi province NW of Beijing (Ohara et al., 2007; Wang et al., 2005), may have contributed significantly to the regional sulfate aerosols observed in Beijing. The Group II backtrajectories indeed passed through those sources.

The lowest NR-PM_1 loading (=21 μg m^{-3}) was observed for the Group I air mass that came from the north. Among all, the Group I trajectory corresponded to the strongest wind speed (>1200 km in distance over the course of 48 h) and its aerosol was composed of the highest fraction of primary aerosol–HOA. Note that NR-PM_1 loadings and BT distances did not correlate in this study. Since there are few direct sources of aerosol or aerosol precursors north of Beijing, the high fraction of HOA indicates a significant contribution of primary emissions in and around the vicinity of Beijing to the aerosol pollution observed during this study.

4. Conclusion

Submicron particles were characterized in urban Beijing with an AMS during 9–21 July 2006. The average ($\pm1\sigma$) concentrations of organics, SO_4^{2-}, NO_3^-, NH_4^+, and Cl^- were 28.1 ± 14.8, 20.3 ± 11.6, 17.3 ± 13.2, 13.1 ± 7.4, and 1.1 ± 1.1 μg m^{-3}, respectively. Organics and sulfate were the dominant species, together accounting for an average 60% of the total NR-PM_1 mass. Nitrate was also an important aerosol component in Beijing, constituting an average 20% of the NR-PM_1 mass. During this study, NH_4^+ and inorganic anions (i.e., SO_4^{2-}, NO_3^-, Cl^-) in NR-PM_1 were under stoichiometric balance, indicating that particles were bulk neutralized. The size distributions of inorganic species were very similar to each other and all peaked at $D_{va} \approx 600$ nm while that of OA showed a pronounced shoulder extending into the ultrafine mode. As a result, particles smaller than 200 nm were mostly organic. The broad OA size distribution reflected contributions of combustion-related POA that is usually enriched in ultrafine particles.

Three OA components were determined with PMF analysis of the AMS organic spectra, including a HOA component likely corresponding to POA material associated with combustion-related emissions, an OOA II likely representative of less oxidized, semi-volatile SOA, and an OOA I that correlated well with sulfate and likely represented more oxidized, regional SOA. Although primary emissions are apparently an important source of aerosol in Beijing, our results indicate that fine particle loading was controlled by secondary species.

Backtrajectory analysis was conducted to evaluate the relative impacts of regional and local sources on the variability in aerosol composition and loading observed during this study. Correlations between aerosol properties and BT profiles suggest that regional transport from regions S and W of Beijing contributed significantly to PM_1 measured in Beijing. This hypothesis is further supported by the fact that secondary species dominated NR-PM_1 composition in Beijing. Nevertheless, our analyses suggest that primary emissions (e.g., traffic) from local sources are an important contributor of PM in Beijing, especially during relatively low loading periods. The

severe aerosol pollution observed during this study was attributed to intense emissions of primary PM and regional production of secondary PM, which were exacerbated by the stagnant meteorological conditions (and thus poor ventilation).

Acknowledgments

This study is supported by the National Natural Science Foundation of China (Grant No. 40575063), National Basic Research Program of China (Grant No. 2006CB403703, 2006CB403701) and the Climate Change Program of China Meteorological Administration. The participation of Qi Zhang and Yele Sun has been supported by the U.S. National Science Foundation (grant ATM-0840673) and the U.S. Department of Energy (grant DE-FG02-08ER64627). The authors gratefully acknowledge Ingrid Ulbrich for the PMF panel and James Allan the standard Q-AMS data analysis software, Guo Xiaoyin for help in drawing Beijing map and sampling site, and the NOAA Air Resources laboratory (ARL) for the provision of the HYSPLIT transport and dispersion model and READY website used in this publication.

Appendix. Supplementary data

Supplementary data associated with this article can be found, in the online version, at doi:10.1016/j.atmosenv.2009.03.020.

References

Alfarra, M.R., et al., 2004. Characterization of urban and regional organic aerosols in the lower Fraser Valley using two aerodyne aerosol mass spectrometers. Atmos. Environ. 38, 5745–5758.

Allan, J.D., et al., 2003. Quantitative sampling using an aerodyne aerosol mass spectrometer. Part 2: measurements of fine particulate chemical composition in two UK cities. J. Geophys. Res.-Atmos. 108 (D3), 4091, doi:10.1029/2002JD002359.

Allan, J.D., et al., 2004a. Submicron aerosol composition at Trinidad Head, California, during ITCT 2K2: its relationship with gas phase volatile organic carbon and assessment of instrument performance. J. Geophys. Res.-Atmos. 109 (D23), D23S24, doi:10.1029/2003JD004208.

Allan, J.D., et al., 2004b. A generalised method for the extraction of chemically resolved mass spectra from Aerodyne aerosol mass spectrometer data. J. Aerosol Sci. 35 (7), 909–922, doi:10.1016/j.jaerosci.2004.02.007.

Canagaratna, M.R., et al., 2004. Chase studies of particulate emissions from in-use New York city vehicles. Aerosol Sci. Technol. 38, 555–573, doi:10.1080/02786820490465504.

Canagaratna, M., et al., 2007. Chemical and microphysical characterization of ambient aerosols with the aerodyne aerosol mass spectrometer. Mass Spectrom. Rev. 26, 185–222, doi:10.1002/mas.20115.

Chan, C.K., Yao, X., 2008. Air pollution in mega cities in China. Atmos. Environ. 42 (1), 1–42.

DeCarlo, P., et al., 2004. Particle morphology and density characterization by combined mobility and aerodynamic diameter measurements. Part 1: theory. Aerosol Sci. Technol. 38, 1185–1205.

Dillner, A.M., et al., 2006. Size-resolved particulate matter composition in Beijing during pollution and dust events. J. Geophys. Res. 111 (D5), doi:10.1029/2005JD006400.

Draxler, R.R., Rolph, G.D., 2003. HYSPLIT (HYbrid Single-Particle Lagrangian Integrated Trajectory). NOAA Air Resources Laboratory, Silver Spring, MD. Model access via NOAA ARL READY Website. <http://www.arl.noaa.gov/ready/hysplit4.html>.

Drewnick, F., et al., 2004. Measurement of ambient aerosol composition during the PMTACS-NY 2001 using an aerosol mass spectrometer. Part I: mass concentrations. Aerosol Sci. Technol. 38 (S1), 92–103.

Duan, F., et al., 2004. Identification and estimate of biomass burning contribution to the urban aerosol organic carbon concentration in Beijing. Atmos. Environ. 38, 1275–1282.

Guinot, B., et al., 2007. Beijing aerosol: atmospheric interactions and new trends. J. Geophys. Res. 112 (D14314), doi:10.1029/2006JD008195.

He, K.B., et al., 2001. The characteristics of PM2.5 in Beijing, China. Atmos. Environ. 35, 4959–4970.

He, K.B., et al., 2002. Urban air pollution in China: current status, characteristics, and progress. Annu. Rev. Energy Environ. 27, 397–431.

Hu, X., et al., 2005. Observational study of wind fields, temperature fields over Beijing area in summer and winter. Universitatis Pekinensis (Acta Scientiarum Naturalium) 41 (3), 399–407.

Lanz, V.A., et al., 2007. Source apportionment of submicron organic aerosols at an urban site by factor analytical modelling of aerosol mass spectra. Atmos. Chem. Phys. 7, 1503–1522.

Matthew, B.M., et al., 2008. Collection efficiencies in an aerodyne aerosol mass spectrometer as a function of particle phase for laboratory generated aerosols. Aerosol Sci. Technol. 42, 884–898.

Ohara, T., et al., 2007. An Asian emission inventory of anthropogenic emission sources for the period 1980–2020. Atmos. Chem. Phys. 7 (16), 4419–4444.

Paatero, P., Tapper, U., 1994. Positive matrix factorization: a non-negative factor model with optimal utilization of error estimates of data values. Environmetrics 5, 111–126.

Salcedo, D., et al., 2006. Characterization of ambient aerosols in Mexico city during the MCMA-2003 campaign with aerosol mass spectrometry: results from the CENICA Supersite. Atmos. Chem. Phys. 6, 925–946. SRef-ID: 1680-7324/acp/2006-6-925.

Sciare, J., et al., 2007. Semi-volatile aerosols in Beijing (R.P. China): characterization and influence on various PM2.5 measurements. J. Geophys. Res. 112 (D18202), doi:10.1029/2006JD007448.

Streets, D.G., et al., 2007. Air quality during the 2008 Beijing Olympic Games. Atmos. Environ. 41 (3), 480–492.

Sun, Y., et al., 2004. The air-borne particulate pollution in Beijing-concentration, composition, distribution and sources. Atmos. Environ. 38, 5991–6004.

Takegawa, N., et al., 2005. Characterization of an aerodyne aerosol mass spectrometer (AMS): intercomparison with other aerosol instruments. Aerosol Sci. Technol. 39 (8), 760–770.

Ulbrich, I., Canagratna, M., Zhang, Q., Worsnop, D., Jimenez, J.L, 2009. Interpretation of organic components from positive matrix factorization of aerosol mass spectrometric data. Atmos. Chem. Phys. 9, 2891–2918.

Varutbangkul, V., et al., 2006. Hygroscopicity of secondary organic aerosols formed by oxidation of cycloalkenes, monoterpenes, sesquiterpenes, and related compound. Atmos. Chem. Phys. 6, 2367–2388.

Wang, X.P., et al., 2005. A high-resolution emission inventory for Eastern China in 2000 and three scenarios for 2020. Atmos. Environ. 39, 5917–5933.

Zelenyuk, A., et al., 2006. Evaporation of water from particles in the aerodynamic lens inlet: an experimental study. Anal. Chem. 78 (19), 6942–6947.

Zhang, Q., et al., 2005a. Deconvolution and quantification of hydrocarbon-like and oxygenated organic aerosols based on aerosol mass spectrometry. Environ. Sci. Technol. 39 (13), 4938–4952, doi:10.1021/es048568l.

Zhang, Q., et al., 2005b. Time and size-resolved chemical composition of submicron particles in Pittsburgh - implications for aerosol sources and processes. J. Geophys. Res. 110, D07S09, doi:10.1029/2004JD004649.

Zhang, Q., et al., 2005c. Hydrocarbon-like and oxygenated organic aerosols in Pittsburgh: insights into sources and processes of organic aerosols. Atmos. Chem. Phys. 5, 3289–3311.

Zhang, Q., et al., 2007a. Ubiquity and dominance of oxygenated species in organic aerosols in anthropogenically-influenced northern hemisphere mid-latitudes. Geophys. Res. Lett. 34, L13801, doi:10.1029/2007GL029979.

Zhang, Q., et al., 2007b. A case study of urban particle acidity and its influence on secondary organic aerosol. Environ. Sci. Technol. 41 (9), 3213–3219.

Zheng, M., et al., 2005. Seasonal trends in PM2.5 source contributions in Beijing, China. Atmos. Environ. 39 (22), 3967–3976.

Zhuang, X., et al., 1999. A study on the severe hot weather in Beijing and North China Part I. Statistics and synoptic case study. Climat. Environ. Res. 4 (4), 323–333.